LAWRENCE
LIVERMORE
NATIONAL
LABORATORY

Dislocation Image Stresses at Free Surfaces by the Finite Element Method

M. Tang, G. Xu, W. Cai, V. Bulatov

November 26, 2003

Disclaimer

Dislocation Image Stresses at Free Surfaces by the Finite Element Method

Meijie Tang, Guanshui Xu*, Wei Cai, Vasily Bulatov,
Lawrence Livermore National Laboratory, P. O. Box 808,
Livermore, CA 94551
* Dept. of Mechanical Engineering, Univ. of California at Riverside,
Riverside, CA 92521

ABSTRACT

The finite element method has been routinely used to calculate the image stresses of dislocation segments. When these segments intersect with surfaces, the image stresses at the surfaces diverges singularly. At the presence of these singularities, both convergence and accuracy of using the finite element method need to be examined critically. This article addresses these issues with the aim toward the application of dislocation dynamics simulations in thin films.

INTRODUCTION

Dislocations in a finite medium have image stresses [1]. Unlike electrostatic systems, the image stress of dislocations can not be straightforwardly obtained by simple image superposition. It is generally recognized that these image stresses play important roles in the dislocation behavior in finite sized systems such as thin films. In recent years, the development of discrete dislocation dynamics simulation [2-3] has made the simulation of thin film plasticity possible, presuming the image stresses can be calculated accurately and efficiently. Typically, the image stresses are calculated using the finite element method (FEM), which is then coupled with a dislocation dynamics method [4-7]. When dislocations intersect with surfaces, the image stresses at the surfaces diverge singularly. At the presence of these singularities, both convergence and accuracy of using the FEM need to be examined critically. This article addresses these issues by performing systematic FEM calculations in simplified systems and to compare with analytical solutions.

METHODOLOGY

The FEM is a standard method to solve boundary value problems [8]. The problem being concerned here is the following: given the elastic stress field of a dislocation segment in an infinite medium, find the elastic field of the dislocation segment in a finite body with a stress-free boundary. The solution takes the form $\sigma_{ij}^{\infty} + \sigma_{ij}^{img}$, where the first term is the stress in the infinite medium, and the second term is the image stress due to the boundary. The image stress can be obtained by FEM through solving the boundary value problem so that the surface traction $\sigma_{ij}^{img} n_j$ cancels the original traction $\sigma_{ij}^{\infty} n_j$ on the surface, where n_j is the component of the normal vector to the surface.
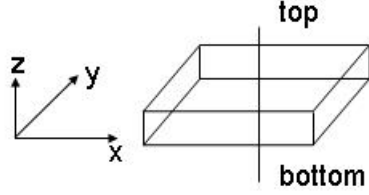
Figure 1. A schematic view of the setup of the calculations. The thin slab has one free surface at the top perpendicular to the z direction. The infinite dislocation is perpendicular to the free surface.

The system being studied is a thin slab with one free surface at the top perpendicular to the z direction, as shown in figure 1. All calculations are done with the dimensions of the slab being 300x300x60 angstroms along x, y, and z directions respectively. An infinite dislocation is located near the center of the slab. It is perpendicular to the free surface. Its location at the free surface is shifted by (+M/4,+M/4) along x and y directions, where M is the mesh size. The FEM code used in the calculations utilizes both direct and conjugate iterative solvers. The later is shown to be much more efficient with large systems containing thousands of elements and more. Homogenous cubic (i.e., brick) meshes are used throughout the calculations. Mesh sizes vary from 6 down to 0.86 angstroms. The smallest mesh that can be used is limited by the largest number of elements a single processor can handle. The largest calculation contained $12.8 x 10^6$ number of elements and the memory usage was nearly 20 giga bytes.

The boundary condition at the free surface is the traction free boundary condition mentioned earlier. Fixed displacement boundary condition is applied at the four side surfaces. Two types of boundary conditions are applied at the bottom surface. One is the fixed displacement boundary condition, which is defined as the type I boundary condition. The other is the application of the known analytical stress boundary condition for a semi-infinite medium. The analytical image stress field for an infinite dislocation perpendicular to the free surface in a semi-infinite medium was worked out by Honda [9]. One then superimposes Honda's solution with the infinite segment stress field and applies the total stress field at the bottom surface. We define this as the type II boundary condition.

The results to be presented next are the image stress values solved by the FEM along the dislocation line inside the slab. The stresses are calculated at the Gaussian points. For simplicity, only the stresses at 1 Gaussian point is sampled which results in constant stresses for each element. Thus, for any point in space, we find out the element where the point resides, and use the element stresses as the calculated stresses at the point.

RESULTS AND DISCUSSIONS

The first set of calculations is done for the slab of 300x300x60 angstroms with the type II boundary condition. The dislocation Burgers vector is along <100>. The only non-zero image stress component on the dislocation line is σ_{yz}, noted as σ. The stresses are shown as scaled values with respect to the shear modulus, and they are calculated at positions with 0.5 angstroms apart from each other. The first point is 0.5 angstroms below the free surface. The Poisson ratio is 0.35 and the Burgers vector is 2.86 angstroms. Figure 2 shows the image stresses calculated by the FEM method with type II boundary condition at the bottom surface and the analytical values, where the same results are plotted differently along the x axis.
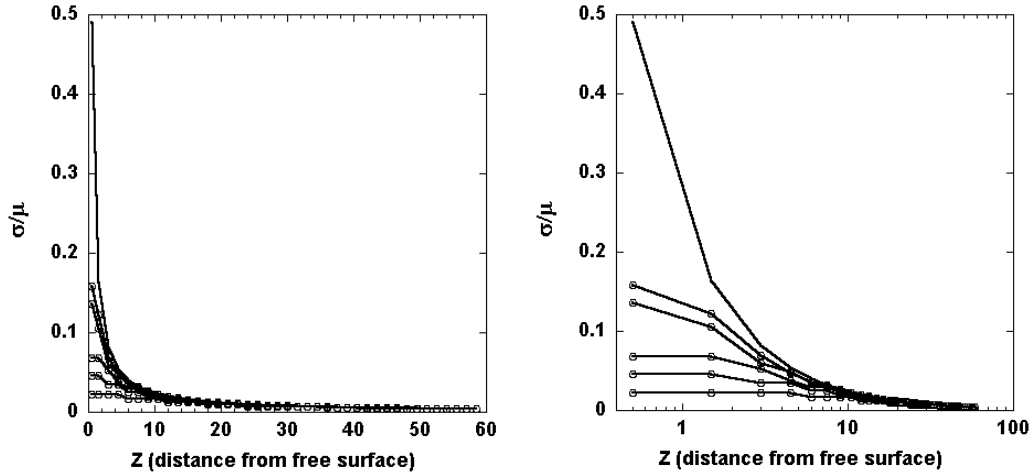
Figure 2. The FEM calculation of the image stresses along the dislocation line. As a comparison, the solid line without symbols is obtained from the analytical solution. For the rest lines with symbols, each corresponds to a different mesh size. The mesh sizes are 6, 3, 2, 1, 0.86 angstroms respectively. (a) Linear plots in x and y; (b) logarithmic plot in x and linear plot in y. Type II boundary condition is applied at the bottom surface.

Figure 2(a) is plotted in linear scale and 2(b) in logarithmic scale in order to view the data close to the free surface more clearly. Along y axis, linear scale is used for both (a) and (b). From the analytical solution, one sees that the image stress close to the free surface is enormous, almost half of the shear modulus of the material being considered. This suggests a potentially important role the image stress may play at the end of the dislocation close to the free surface. This effect can manifest itself into important significance to affect the overall dislocation behavior. The FEM calculations do show convergence as the mesh size is decreased. However, even with the smallest mesh possible, the values close to the surface have a rather large systematic error compared to the analytical value. The farther away from the free surface, the faster the results converge and the better agreement with the analytical values. This is expected since the image stress varies as 1/r from the free surface.
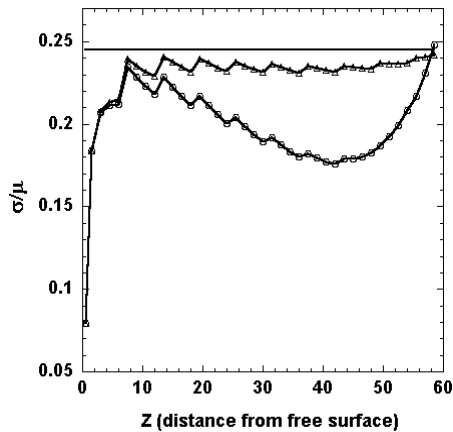

Figure 3. Comparison of type I and type II boundary conditions at the bottom surface. The line with square symbols is obtained using type I boundary condition and the line with square symbols is obtained using type II boundary condition. The solid line without symbol is the analytical result. The FEM calculations are done with the mesh size of 0.86 angstroms.

Similar calculations are done for type I boundary condition at the bottom surface. Figure 3 shows the comparison between the two types of boundary conditions and the analytical

results. The results are plotted for the multiplication of the stress and the distance from the free surface, i.e., $\dfrac{\sigma \cdot z}{\mu}$, instead of $\dfrac{\sigma}{\mu}$. The analytical result is a straight line because the stress varies as 1/r from the free surface. The type II boundary condition results agree well with the analytical ones except when approaching the free surface. The type I boundary condition results show rather large deviation from the analytical solution. This indicates a boundary effect due to the bottom surface. However, the results using type I and II boundary conditions become identical within about 8 angstroms from the free surface. This means that the boundary condition at the bottom surface has no effect to the results close to the free surface. This means that the image stress close to the free surface is largely determined by the free surface only.

CONCLUSION

The image stresses of a dislocation in a finite medium are calculated using the finite element method. The results are compared to the analytical solution. Although the finite element method results indicate convergence towards the analytical solution, the mesh sizes required to achieve the satisfactory convergence would be too small for the practical application of the FEM in dislocation dynamics simulation. Although it is a fundamentally sound and generally effective approach to couple the FEM with the dislocation dynamics simulations to deal with image stresses, the accuracy of the method is largely limited by the treatment of the singular stress field at the intersection of the dislocation segment and the surface of the boundary. As shown in the present paper, by refining mesh size is not satisfactory for practical applications of the dislocation dynamics simulations. We can conclude that it is highly unrealistic to enforce the rigorous boundary conditions of dislocation dynamics simulations in finite systems by using the finite element method alone. To overcome this difficulty, we have pursued a hybrid method in which the general analytical solutions of dislocation segments in a semi-infinite medium are used to treat the singular part of the image stress field. The moderate non-singular part of the image stress field of dislocation segments can then be treated with the finite element method using much coarser meshes. The effectiveness of this approach is being studied [10].

ACKNOWLEDGMENTS

REFERENCES

1. J. P. Hirth and J. Lothe, Theory of dislocations, 2nd ed., Wiley, New York, NY (1982).
2. V. V. Bulatov, M. Tang, and H. Zbib, MRS Bulletin **26**, 191(2001).
3. M. Tang, L. P. Kubin, and G. R. Canova, G. R., Acta Meta., **46**, 3221(1998).
4. E. Van der Giessen and A. Needleman, Computational Materials Modeling **42**, 294 (1994).

5. M. C. Fivel, T. J. Gosling, and G. R. Canova, Modelling Simul. Mater. Sci. Eng. **7**, 753 (1999).
6. R. Martinez and N. M. Ghoniem, Comp. Model. Eng. Sci. **3**, 229 (2002).
7. S. Groh, B. Devincre, L. P. Kubin, A. Roos, F. Feyel, J-L. Chaboche, Phil. Mag. Lett. **83**, 303 (2003).
8. Thomas J. R. Hughes, The Finite Element Method: linear static and dynamic finite element analysis, Dover Publications Inc., Mieola, New York (2000).
9. K. Honda, Jap. J. Appl. Phys. **18**, 215 (1979).
10. M. Tang, W. Cai, V. Bulatov, G. Xu, to be published.